Chapter 4

A Cross-Coupling Approach for the Synthesis of the Enmein-Type Ent-Kauranoids[†]

4.1 INTRODUCTION

While there have been a number of elegant syntheses of ent-kauranoid natural products by our group and others, we felt that the compelling structure and promising biological activity of these natural products warranted further investigation. While there have been several creative strategies toward the synthesis of these natural products, we felt that a more convergent assembly of the kauranoid core would greatly improve upon the existing strategies. A convergent and easily diversifiable synthetic approach to these natural products will allow access to several of these highly oxygenated terpenes and enable an in-depth investigation of the structure-activity relationship (SAR).

[†] The research discussed in this chapter was completed in collaboration with Kelsey E. Poremba, a graduate student in the Reisman Lab.

4.2 SYNTHETIC STRATEGY

4.2.1 Retrosynthetic Analysis

In considering the structure of the enmein-type *ent*-kauranoids (e.g. **301**), we identified the central B-ring lactone as a strategic ring forging junction for two bicyclic systems. Conceptually, we thought to cleave the molecule through the B ring, revealing two fragments of similar size and complexity (**402** & **403**) (Scheme **4.1a**). We were excited at the prospect of using an epoxy alcohol (**402**) as our A/C-ring fragment, as we felt that we could apply reductive cyclization chemistry our lab had investigated in the total syntheses of **292**, **293**, and **295** (Scheme **4.1b**).[1–3] Our lab found that reductive opening of epoxide **368**, followed by intermolecular trapping by Michael acceptor **404** could enable spirocycle formation, delivering **369** in excellent yield as a single diastereomer.

Scheme 4.1 *A simplifying convergent strategy to access **301**.*

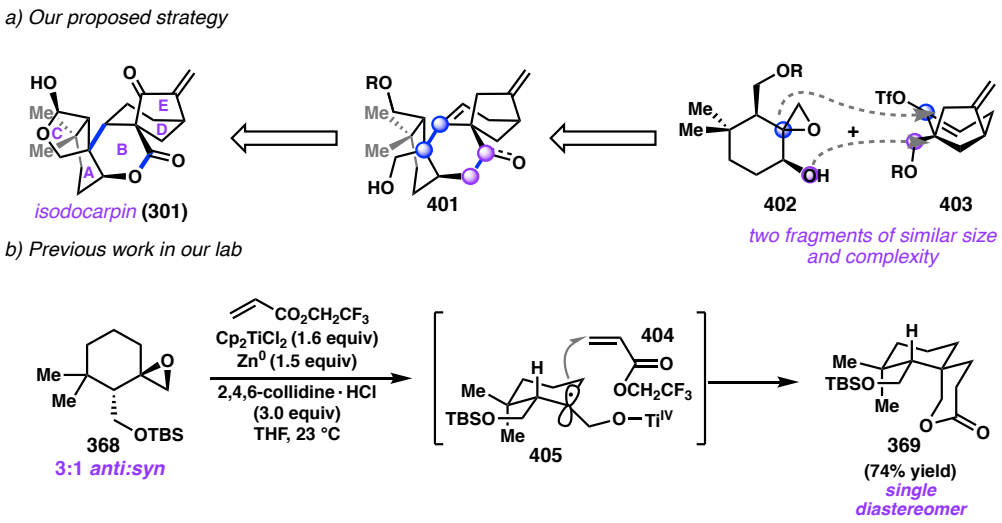

We hypothesized that we could use a similar substrate (**402**), but instead of engaging the resulting tertiary radical in a Giese-type addition to an acrylate, use a Ni-

catalyzed intermolecular epoxide alkenylation to join the two fragments (Scheme **4.1a**). This transformation would leverage a similar carbon-centered radical intermediate our lab used in prior syntheses, but would seek to increase the convergence and modularity of the synthesis through the direct coupling of a bicyclic alkenyl triflate (**403**). In addition, this convergent coupling strategy would allow us to vary the oxidation pattern on either fragment, thereby providing modular access to other *seco-ent*-kauranoids.

Scheme 4.2 *First generation retrosynthesis of the enmein-type ent-kauranoids.*

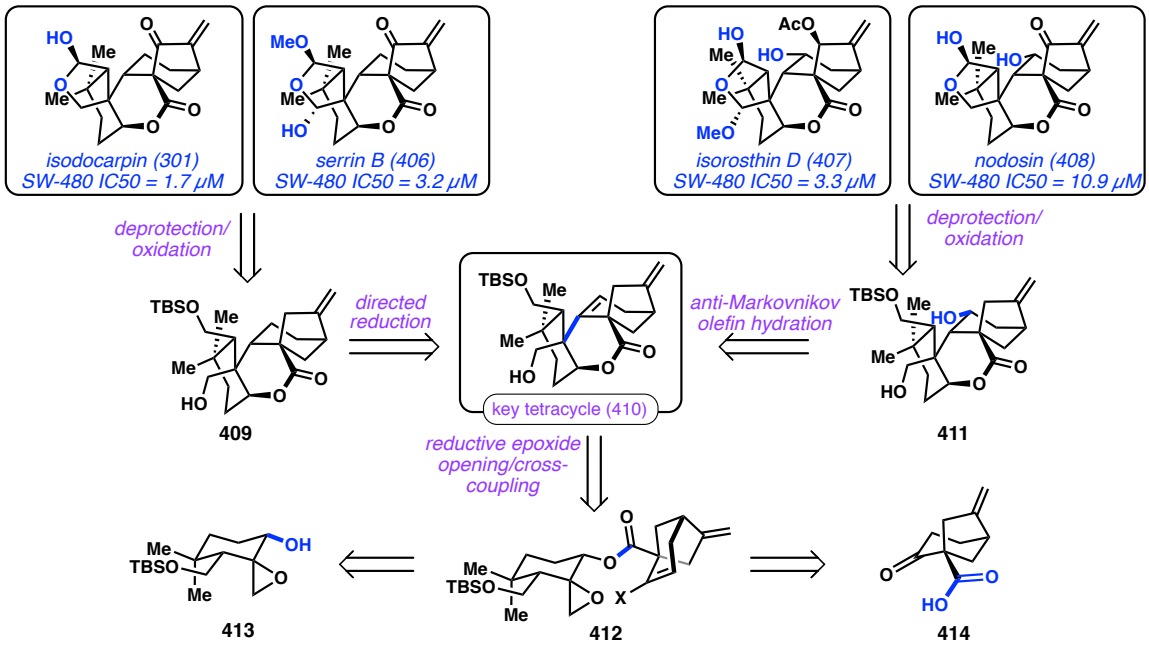

Retrosynthetically, we envisioned that we could access four natural products through a unified strategy (Scheme **4.2**). Isodocarpin (**301**) and serrin B (**406**) could be accessed through a deprotection/oxidation sequence of lactone **409**. We hypothesized that **409** could arise from a directed reduction of the tetracycle **410**. Similarly, isorosthin D (**407**) and nodosin (**408**) could be prepared in an analogous fashion through a deprotection/oxidation sequence of diol **411**. We envisioned preparing diol **411** through an

anti-Markovnikov hydration of tetracycle **410**. Disconnection of **410** through the central B-ring lactone would greatly simplify our strategy. We hypothesized that we could prepare **410** through formation of the key C–C bond (shown in blue) via an intramolecular, reductive-epoxide opening/cross-coupling reaction of **412**. The substrate for this key cyclization reaction could be obtained through ester bond formation between two appropriately functionalized building blocks: epoxy alcohol **413** and [3.2.1]-bicyclooctane **414**. While previous studies toward the synthesis of 6,7-seco-*ent*-kauranoids have relied upon linear syntheses, this convergent coupling strategy will provide an efficient and expedient preparation of these oxygenated terpenoids with a modular approach that will potentially allow for the introduction of varying functionality on each coupling fragment.

4.2.2 Reductive Cross-Coupling of Epoxides

In addition to the work our lab has done in the field of reductive cross-electrophile coupling,[4–9], we were also inspired by a number of reactions reported by the Weix and Gong groups that could be explored further to achieve our desired cross-coupling. In 2014, Weix and coworkers reported a cross-coupling reaction enabled by nickel and titanium co-catalysis, providing the Markovnikov reductive arylation products between epoxides and aryl halides (Scheme **4.3a**).[10] In 2015, they expanded upon this methodology; by using a chiral titanocene, they could render this transformation asymmetric, enabling a desymmetrization of cyclic *meso*-epoxides (Scheme **4.3b**).[11] It is of note that in this reaction they were able to successfully employ alkenyl bromides and alkenyl triflates as cross-coupling partners, providing encouraging precedent for our desired transformation.

Scheme 4.3 *Precedent for desired cross-electrophile coupling.*

(a) Ni-catalyzed reductive cross-coupling of epoxides (Weix, 2014)

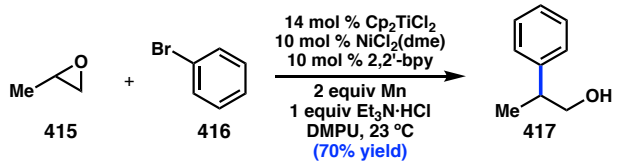

(b) Asymmetric reductive cross-coupling of epoxides (Weix, 2015)

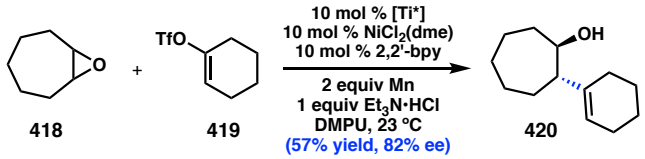

(c) Ni-catalyzed reductive cross-coupling to form quaternary centers (Gong, 2015)

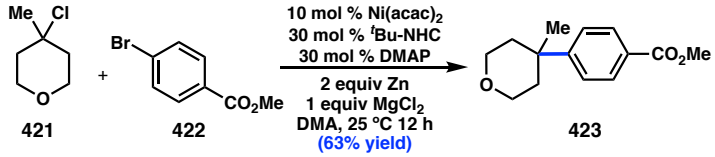

Although the epoxide coupling we have proposed has not yet been employed to form quaternary centers, Gong and coworkers have demonstrated that quaternary centers can be generated through related Ni-catalyzed reductive cross-coupling reactions (Scheme **4.3c**).[12] To date, all previously reported epoxide cross-couplings have been developed on relatively simple systems, to form C–C bonds at secondary stereogenic centers, and there have been no demonstrated applications to complex natural product synthesis. Given the myriad methods for the preparation of epoxides, as well as the high levels of stereocontrol observed in the variety of epoxidation methods, we anticipate that the development of the proposed convergent fragment coupling would provide a new tool for complex natural product synthesis.

Scheme 4.4 *Mechanistic proposal for reductive cross-coupling.*

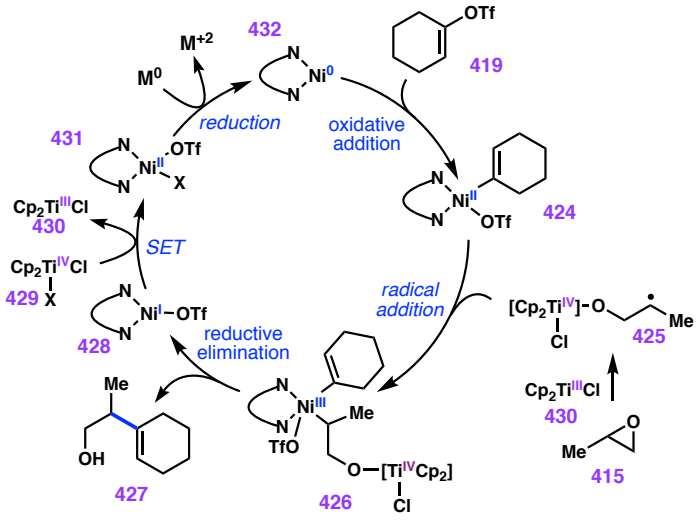

A proposed mechanism for the Ni/Ti co-catalyzed reductive cross-coupling of epoxides is shown in Scheme **4.4**. Oxidative addition of enol triflate **419** to Ni(0) provides a Ni(II) alkenyl species **424**. Ti(III) species **430** generated from the reduction of the Ti(IV) pre-catalyst by a stoichiometric metal reductant can homolytically activate epoxide **415** to deliver the more substituted carbon centered radical **425**. Addition of radical **425** to LNi(II)R_{vinyl}OTf complex **424** provides Ni(III) complex **426**, which can undergo facile reductive elimination to produce **427**. SET between the resultant LNi(I)OTf complex **428** and Cp^2Ti(IV)ClX species **429** would regenerate the active Cp_2Ti(III)X reductant **430**, as well as LNi(II)X_2 complex **431** that can undergo reduction by the stoichiometric reductant to close the catalytic cycle. Thus, productive cross-coupling requires matching of the relative rates of the enol triflate oxidative addition and the epoxide opening, such that adequate concentrations of LNi(II)R_{vinyl}OTf (**424**) and radical **425** are present to engage in a bimolecular reaction step.

4.2.3 Investigation of an Intramolecular Cross-oupling

4.2.3.1 Epoxy Alcohol Synthesis

In our preliminary studies, we developed a first-generation synthesis of epoxide **413**, shown in Scheme **4.5**. Our synthesis commenced with material from the chiral pool. Epoxidation of α-cyclogeraniol (**433**) using mCPBA as the oxidant delivered a single diastereomer of the epoxy alcohol **434**, which could be silylated under standard conditions to provide **435**.[13] Epoxide opening utilizing LiTMP and Et_2AlCl afforded allylic alcohol **436** as a single isomer. At this point, a second epoxidation using mCPBA delivered **413**, completing the synthesis of the first coupling fragment. The stereochemistry of the epoxide was determined through 2D NMR experiments. This sequence has been performed on a multi-gram scale to deliver ample quantities of enantiopure **413**.

Scheme 4.5 *Synthetic route to epoxy alcohol* ***413***.

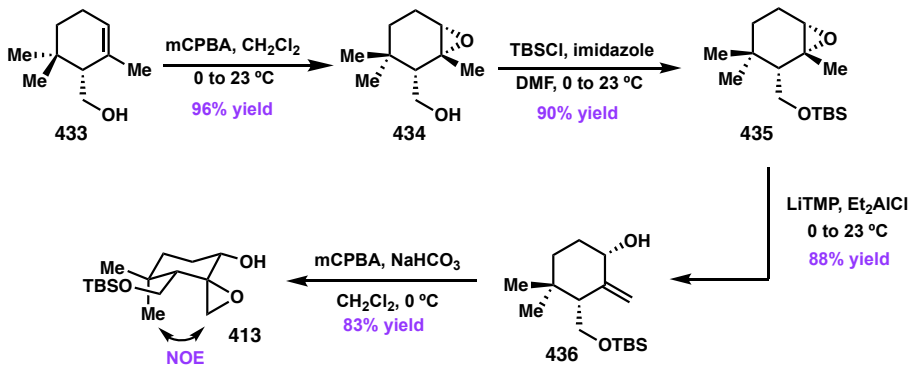

4.2.3.2 [3.2.1]-Bicyclooctanoic Acid Synthesis

With **413** in hand, we turned our attention toward the synthesis of the structurally requisite bicyclo[3.2.1]octane (**414**). While we hoped to develop an asymmetric synthesis of **414**, we were interested in rapidly probing the key step of our synthesis. To this end, we

adapted work from the Snider lab in which structurally-complex bicyclo[3.2.1]octanes could be prepared by a radical polyene cyclization (Scheme **4.6**).[14]

Scheme 4.6 *Synthesis of a bicyclo[3.2.1]octanoic acid.*

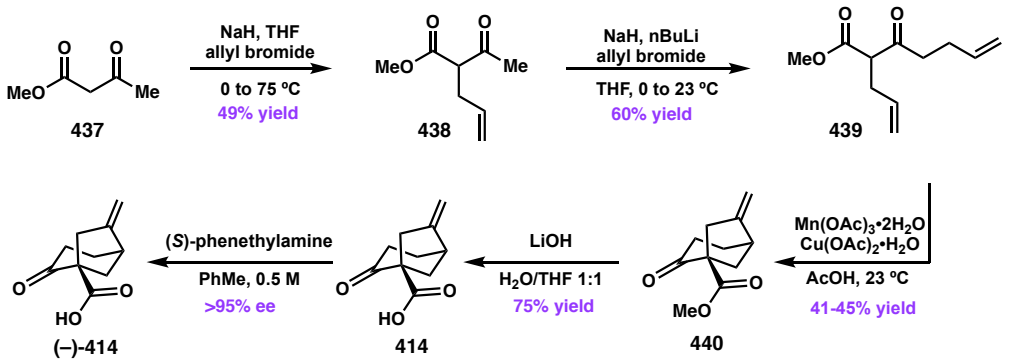

Allylation of the methylene provides methyl 2-acetylpent-4-enoate (**438**), which is subjected to a second allylation to provide **439**. Treatment of **439** with superstoichiometric amounts of $Mn(OAc)_3•2H_2O$, employing $Cu(OAc)_2•H_2O$ as the terminal oxidant, delivered **440** in moderate yield on a three-gram scale. Ester **440** could be hydrolyzed to the carboxylic acid and resolved using (*S*)-phenethylamine by sequential recrystallizations. While we were ultimately interested in preparing **414** directly through an asymmetric transformation, the route depicted in Scheme **4.6** provides rapid access to bicyclo[3.2.1]octanes of structure **414**, which could be used to determine the feasibility of the key epoxide-opening cross-coupling.

4.2.3.3 A Convergent Esterification

We were pleased to see that acylation of the epoxy alcohol **413** with a model neopentyl acyl chloride provided the pivalate ester **441** in excellent yield (Scheme **4.7**). However, attempts to perform the analogous esterification with **442**, generated from our bicyclic acid **414**, were largely unsuccessful. The reaction was plagued by low conversion,

and any attempts to increase the temperature or add additional DMAP resulted in decomposition of starting material.

Scheme 4.7 *Initial attempts at a convergent esterification.*

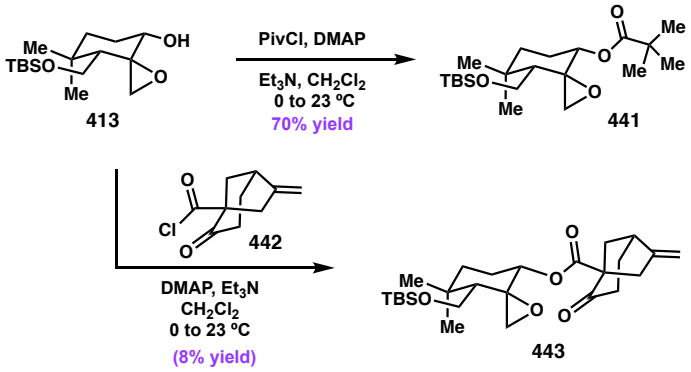

At this point, we turned our attention toward exploring alternative acylation conditions with a commercially available model system, as **414** required multiple steps and a low-yielding resolution sequence. While the use of pivaloyl chloride did not appear to be reflective of the reactivity of **442**, we thought that a bicyclic terpene could serve as a good surrogate to identify how a sterically bulky group could influence the nature of this esterification chemistry. We elected to use ketopinic acid, as we felt its steric bulk matched that present in **414** and was commercially available as a single enantiomer.

We were pleased to see that preparation of a mixed anhydride derived from the coupling of **444** with 2,4,6-trichlorobenzoyl chloride (**446**), followed by trapping with **413** delivered good yields of **445**.[15] Alternatively, treatment of **444** with 2-Me-6-NO_2-benzoic anhydride, followed by trapping with **413,**[16] also provided improved conversion to ester **445** (Table **4.1**). Formation of the mixed anhydride through the coupling of **444** and

isobutyl chloroformate (entry 3) and preparation of the acid chloride (entry 4) resulted in decomposition of starting material.

Table 4.1. *Esterification with a model system.*

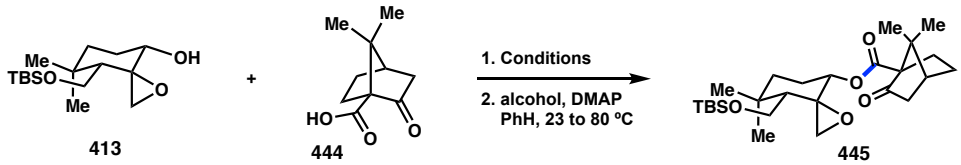

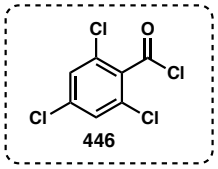

entry	conditions	result
1	446, Et_3N, THF	73% yield
2	2-Me-6-NO_2-benzoic anhydride Et_3N, THF	69% yield
3	$iBuO_2CCl$, Et_3N, THF	decomposition
4	$(COCl)_2$, DMF, PhH	decomposition

After investigating the acylation with the ketopinic acid model (**444**), we turned our attention toward testing these conditions with resolved bicyclic acid **414**. Formation of the mixed anhydride under Yamaguchi conditions, followed by treatment with **413** cleanly delivered **443** in excellent yield on a synthetically useful scale (Scheme **4.8**). We were pleased to see that not only did the esterification proceed smoothly, but conversion to the enol triflate cleanly delivered **447**.[17]

Scheme 4.8 *Preparation of an intramolecular cross-coupling substrate.*

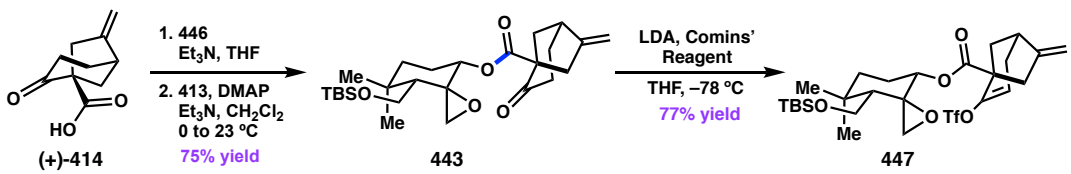

With **447** in hand, we were eager to examine the conditions reported by Weix and coworkers on our system.[10,11] We first set out to investigate how different stoichiometric reductants would influence the reactivity in this particular transformation. Unfortunately, we found that under their standard conditions with a series of different reductants, we were

unable to isolate the desired product, **448** (Table 4.2). We observed solely protodetriflation to provide **450** with manganese as the reductant (Table **4.2**, entry 1). With other reductants, such as Zn^0 and Sm^0, we observed protodetriflation as well as allylic alcohol **449**. After careful review of these results, we hypothesized that the ester linkage may be problematic in this particular transformation.

Table 4.2. *Intramolecular cross-coupling screen.*

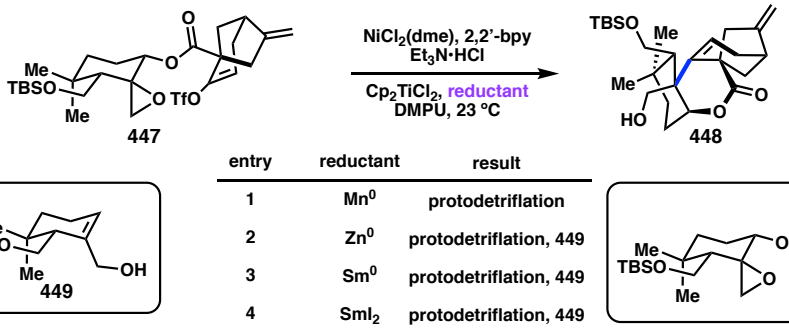

entry	reductant	result
1	Mn^0	protodetriflation
2	Zn^0	protodetriflation, 449
3	Sm^0	protodetriflation, 449
4	SmI_2	protodetriflation, 449

Our investigations indicated that our reaction was being plagued by two problems. First, while we were confident that our nickel catalyst was engaging with our enol triflate, we hypothesized that our substrate was favoring the thermodynamically favored *S*-trans conformation (**452**) rather than the *S*-cis conformation (**451**) required for radical capture of the tertiary radical generated (Scheme **4.9**). Epoxide reduction of **452**, produced radical **453**, with the radical far from the nickel center, making a radical capture process intractable. It seemed that with some reductants, while the epoxide could be successfully reduced, the resulting radical formed adjacent to the ester moiety was unstable, readily decarboxylating to provide **449** and **454**. While we were unable to isolate any side-products from the bicyclic fragment, we hypothesized that **454** could further decompose to give a handful of volatile products that would be difficult to characterize.

Scheme 4.9 *Mechanistic hypothesis for intramolecular cross-coupling.*

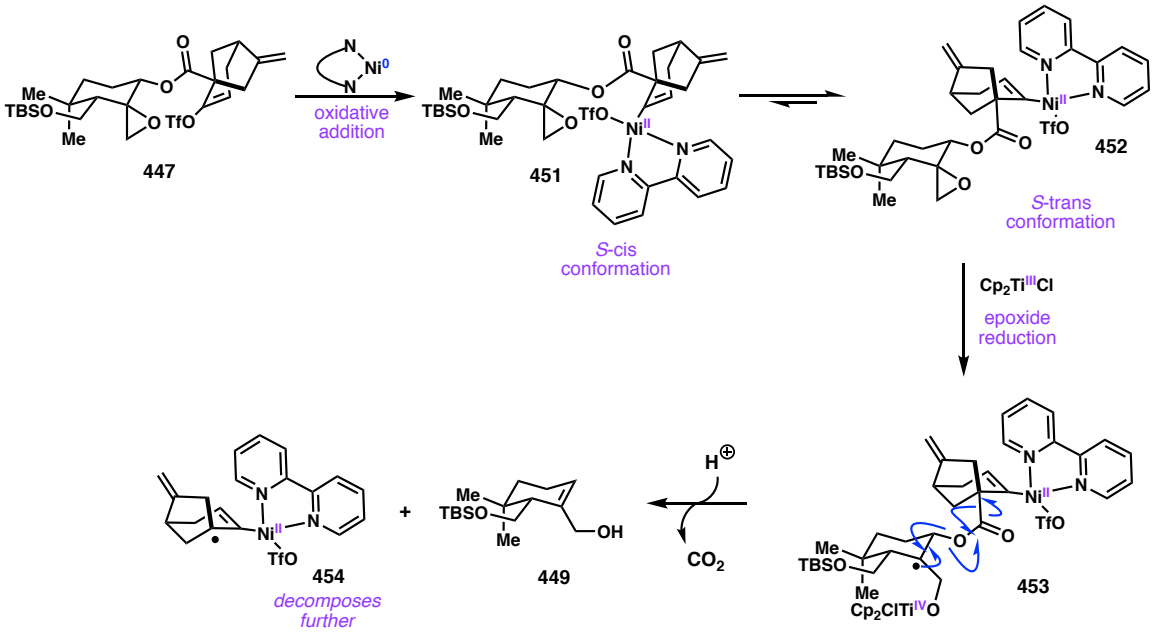

4.2.4 Investigation of an Intermolecular Cross-coupling

4.2.4.1 A Second Generation Retrosynthetic Analysis

Having identified some of the challenges associated with an intramolecular cross-coupling approach for the synthesis of the enmein-type *ent*-kauranoids, we wondered if an intermolecular approach would be more successful. We envisioned carrying out a similar endgame, where **301**, **406**, **407**, and **408** could be accessed from the same key tetracyclic intermediate **410**. However, we envisioned disconnecting through the lactone at this step, to provide diol **455** (Scheme **4.10**). At this point, formation of the all-carbon quaternary center through a convergent cross-coupling simplified the synthesis of **455** to the convergent fragment coupling of **413** and **456**. We felt that attempting this coupling in the intermolecular sense could circumvent some of the issues we encountered in the development of an intramolecular cross-coupling of **447**.

Scheme 4.10 *A second generation retrosynthesis.*

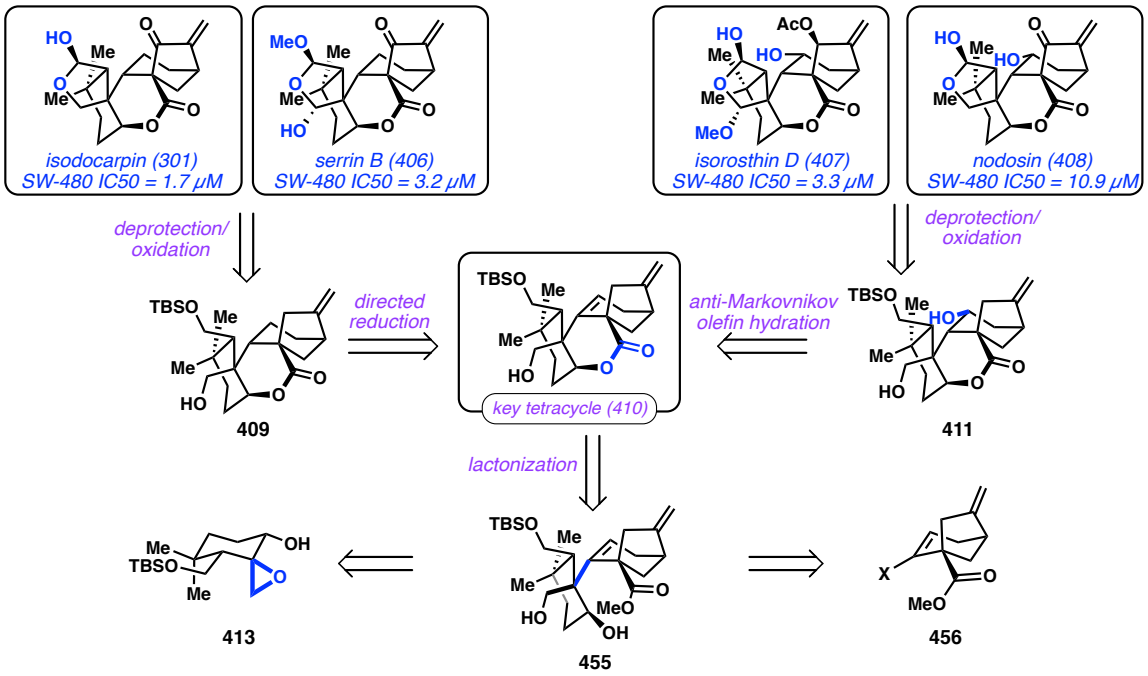

While we had already successfully completed a synthesis of epoxy alcohol **413**, we elected to begin our investigation of this key cross-coupling with a model system for the other cross-coupling partner. We were aware that this would be a difficult reaction to develop, as we knew that reductive cross-couplings with epoxides had not yet been used to generate all-carbon quaternary centers. As such, we felt it would be best to begin with a less complex system. At this point, it was unclear which alkenyl electrophiles would be most successful in the cross-coupling, so we hoped to use a more general system to explore this chemistry. We were also interested in getting preliminary reaction data as quickly as possible, and we knew that the synthesis of **416** would require additional reaction development. Additionally, **414** was only accessible in enantiopure form through a time-

intensive classical resolution, so working with a more easily accessible cross-coupling partner would be ideal.

4.2.4.2 Screening an Intermolecular Cross-coupling

We were pleased to see that we could readily access an enol triflate, alkenyl bromide, and alkenyl iodide from cyclohexanone **458** using a known Stille cross-coupling (Scheme **4.11**).[18] While Weix's reaction worked with enol triflates and alkenyl bromides (Scheme **4.3**), we were excited by the prospect of being able to carefully tune the reactivity of the alkenyl electrophile.

Scheme 4.11 *Synthesis of model C(sp^2) electrophiles.*

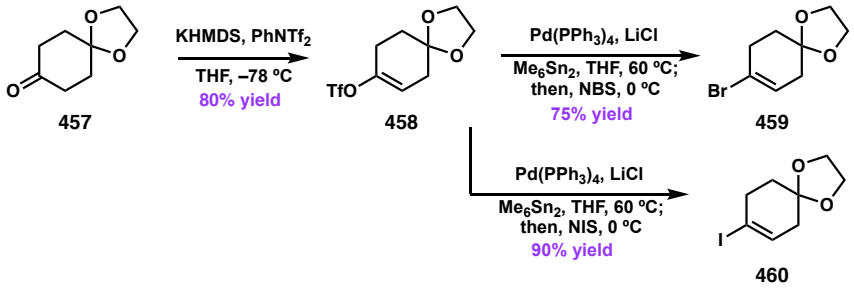

With **458** in hand, we were eager to begin exploring the feasibility of an intermolecular cross-coupling. We began our investigations using epoxy alcohol **413** and enol triflate **458** as the cross-coupling partners and explored different combinations of pyridine ligands and heterogeneous reductants (Table **4.3**). We found that when we used dtbpy, terpy, or phen as the ligand, we observed significant amounts of the epoxide reduction product **462**, regardless of which reductant was employed. Interestingly, we found that the C(sp^2) coupling partner was fully consumed with dtbpy or phen as the ligand, producing significant quantities of the divinyl side-product **463** (entries 1–2, 4–6). When terpy was used, we did not observe any divinyl production (entries 3–4). While we were

not observing any formation of **461**, we were pleased to see that under the reaction conditions we explored, we were observing engagement of both electrophiles, and so we turned our attention to exploring the more reactive alkenyl iodide (**460**) in the reaction.

Table 4.3. *Cross-coupling between an epoxy alcohol and a cyclic enol triflate.*

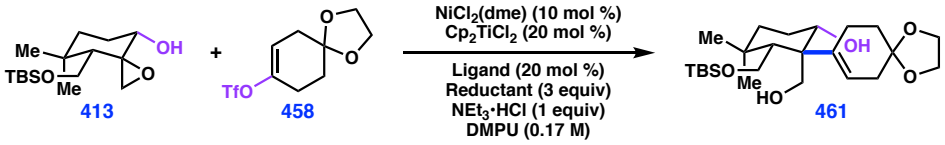

Entry	Ligand	Red.	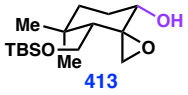 413	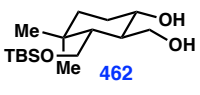 462	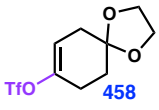 458	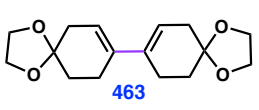 463
1	dtbpy	Mn	26 %	16 %	0 %	15 %
2	dtbpy	Zn	70 %	6 %	0 %	32 %
3	terpy	Mn	17 %	18 %	19 %	0 %
4	terpy	Zn	39 %	14 %	51 %	0 %
5	phen	Mn	15 %	42 %	0 %	7 %
6	phen	Zn	64 %	31 %	0 %	61 %

Unfortunately, we observed similar results when we used alkenyl iodide **460** as the C(sp^2) coupling partner (Table **4.4**); however, we were never able to recover the alkenyl iodide—instead our mass balance shifted toward the protodeiodinated product **464** (entries 1–6). All three ligands delivered significant quantities of the epoxide reduction product **462**, regardless of which reductant was used.

While Weix and coworkers had been successful with pyridine ligands, it seemed as though this class of ligands were not appropriately matched with our particular combination of epoxide and alkenyl electrophile. With this in mind, we began investigating alternative ligand classes that our lab had used in the optimization of other reductive cross-coupling reactions. We were particularly interested in modification of the nickel catalyst

through incorporation of a bis(oxazoline) ligand, as we felt a wider bite angle could facilitate the cross-coupling of more sterically-hindered electrophiles.

Table 4.4. *Cross-coupling between an epoxy alcohol and a cyclic enol triflate.*

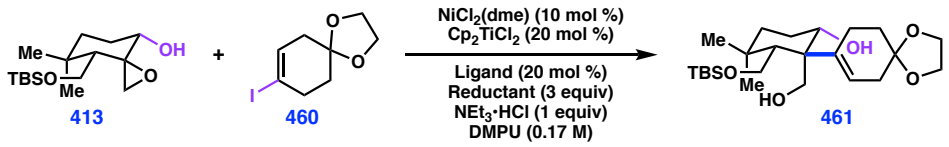

Entry	Ligand	Red.	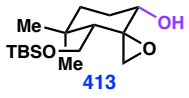 413	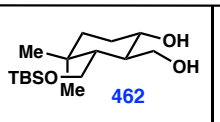 462	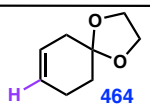 464	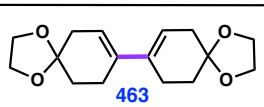 463
1	dtbpy	Mn	12 %	43 %	7 %	70 %
2	dtbpy	Zn	23 %	37 %	10 %	49 %
3	terpy	Mn	28 %	13 %	30 %	0 %
4	terpy	Zn	29 %	12 %	15 %	0 %
5	phen	Mn	48 %	17 %	11 %	21 %
6	phen	Zn	66 %	3 %	5 %	20 %

With this in mind, we began exploring the intermolecular cross-coupling between **413** and enol triflate **458** with the same precatalyst, solvent, reductant, and additives reported by the Weix lab, but with a series of different oxazoline-derived ligands our lab had previously worked with. Unfortunately, none of the ligands screened delivered the desired product, and we observed similar mass-balance as we had seen previously with the pyridine ligands (Table **4.5**). All of the ligands we explored with the exception of *i*-PrOX (entry 6) and *t*-BuQuinOX (entry 8) provided the epoxide reduction product **462**. With regard to the C(sp^2) electrophile, we observed a combination of recovered starting material and divinyl (**463**) with BnBOX and BnPyOX (entries 1 and 5), only recovered starting material with PyBOX, *i*-PrOX, and *t*-BuPHOX (entries 4, 6–7), and only divinyl (**463**) with BOX and *i*-PrCH_2BiOX (entries 2–3).

Table 4.5. *Ligand screening for intermolecular cross-coupling.*

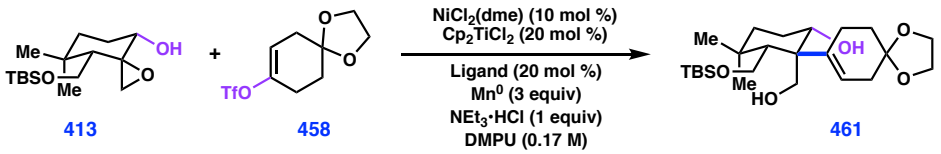

Entry	Ligand	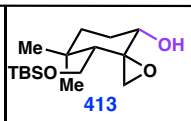 413	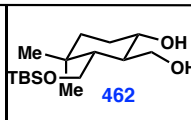 462	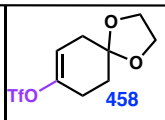 458	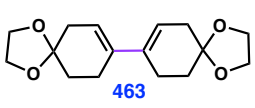 463
1	BnBOX	44 %	22 %	61 %	8 %
2	BOX	25 %	43 %	0 %	22 %
3	iPrCH$_2$BiOX	62 %	11 %	0 %	38 %
4	PyBOX	45 %	26 %	71 %	0 %
5	BnPyOx	44 %	19 %	12 %	31 %
6	iPrOX	67 %	0 %	38 %	0 %
7	tBuPHOX	15 %	51 %	75 %	0 %
8	tBuQuinOx	60 %	0 %	0 %	9 %

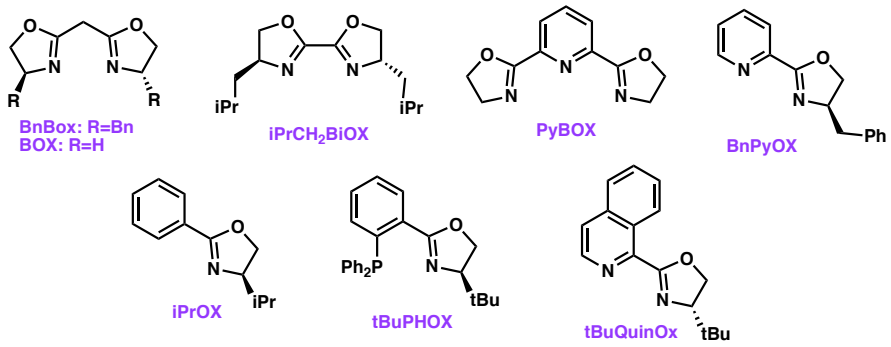

Disappointed that we did not observe the desired reactivity by tuning the employed ligand, we chose to examine the epoxide substrate. We hypothesized that the reduction product **462** was forming due to the slow radical capture by the sterically hindered nickel catalyst, resulting in a high steady state concentration of a radical intermediate, which could be reduced a second time prior to capture by the nickel. In an attempt to stabilize the radical intermediate, we prepared **465**, with an adjacent ketone that we believed could stabilize the intermediate radical species (Scheme **4.12**).

Scheme 4.12 *A resonance-stabilized intermediate.*

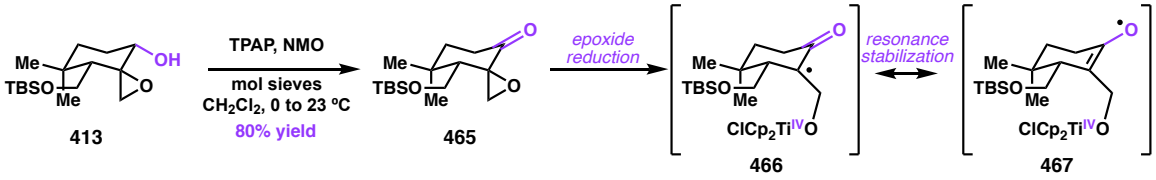

With a stabilized substrate in hand, we returned to the Weix conditions hoping to now observe the desired reactivity. Unfortunately, none of the pyridine ligands we tried provided the desired alkenylated product (Table **4.6**). Interestingly, we observed a new side product, which we identified as the elimination product, producing an exocyclic enone **469** in each of the reactions we examined. However, when we used the enol triflate (**458**) with the epoxy ketone (**465**) rather than the epoxy alcohol (**413**), we observed little to none of the divinyl side-product (**463**). The rest of the mass balance was starting material and decomposition.

Table 4.6. *Cross-coupling between an epoxy alcohol and a cyclic enol triflate*

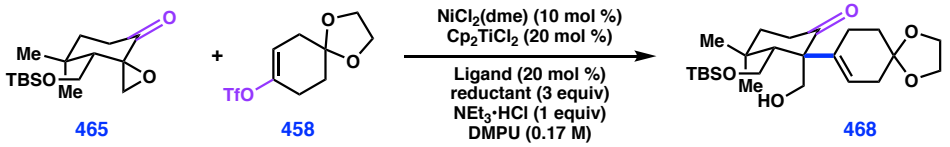

Entry	Ligand	Red.	465	469	458	463
1	dtbpy	Mn	53 %	11 %	81 %	0 %
2	dtbpy	Zn	31 %	23 %	23 %	0 %
3	terpy	Mn	41 %	22 %	66 %	0 %
4	terpy	Zn	59 %	21 %	54 %	0 %
5	phen	Mn	— %	— %	— %	— %
6	phen	Zn	63 %	18 %	2 %	2 %

We hypothesized that while we had increased the stability of the resulting radical, enol radical reduction was outcompeting radical capture by the nickel catalyst, and instead of being reduced again and protonated, **467** was reduced to give enolate **470** and eliminated to produce **469** (Scheme **4.13**). Based on the lack of divinyl produced here, we wondered if the equivalent of hydroxide that was generated from the elimination was inhibiting the catalyst, making it difficult for the catalyst to engage with the enol triflate electrophile.

Scheme 4.13 *Hypothesized formation of side product* ***469***.

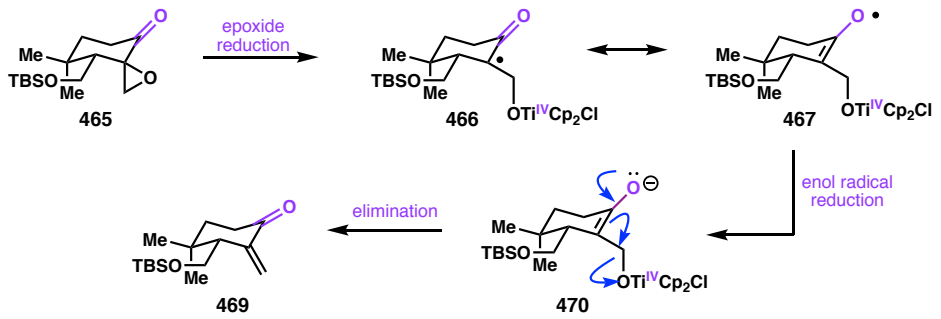

After exploring the cross-coupling between the epoxy ketone **465** and cyclic enol triflate **458**, we also looked at analogous reactions with the more reactive alkenyl iodide (**460**), hoping that by employing a more reactive cross-coupling partner, we would observe better reactivity. Unfortunately, under these conditions, we observed a very similar mass balance, with formation of enone **469** observed in each reaction (Table **4.7**). With regard to the C(sp^2) cross-coupling partner, we observed some formation of the divinyl side-product with the dtbpy ligand (entries 1–2), substantial formation of the divinyl product with the phen ligand (entries 5–6), and only alkenyl iodide with the terpy ligand (entries 3–4). With these findings, it seemed as though using an epoxide substrate designed to stabilize the intermediate radical species was not going to be a viable path forward.

Table 4.7. *Cross-coupling between an epoxy alcohol and a cyclic alkenyl iodide*

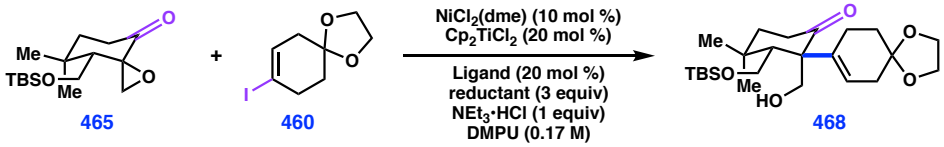

Entry	Ligand	Red.	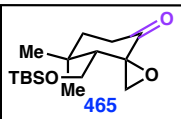 465	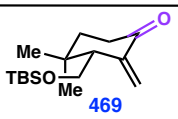 469	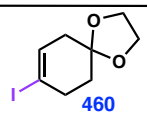 460	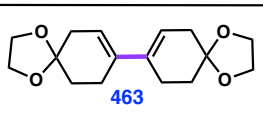 463
1	dtbpy	Mn	31 %	21 %	44 %	6 %
2	dtbpy	Zn	41 %	18 %	57 %	3 %
3	terpy	Mn	43 %	25 %	75 %	0 %
4	terpy	Zn	16 %	36 %	32 %	0 %
5	phen	Mn	33 %	22 %	11 %	39 %
6	phen	Zn	28 %	23 %	0 %	49 %

Unable to produce the desired product with any of the conditions we explored, we wondered if returning to an epoxide that had been reduced *in situ* and engaged in a radical addition reaction would be instructive. In our lab's synthesis of **292**, we treated **368** with a stoichiometric reductant and trapped the resulting radical in a Giese-type addition reaction to forge an all-carbon quaternary center (Scheme **4.1b**). While the enmein-type ent-kauranoids require oxidation on the cyclohexane framework, we wondered if we could use **368** as a substrate to get a handle on some of the chemistry.

While epoxide **368** homolyzed readily with stoichiometric titanocene, we did not observe any of this reactivity under the dual-catalytic conditions (Table **4.8**). In each case, we were able to recover significant amounts of starting material, with none of the reduction product **472** observed. With regard to the C(sp^2) electrophile, we observed complete conversion to the divinyl side product **463** when we used dtbpy or phen as the ligand (entries 1–2, 5–6) and did not observe any conversion with the terpy ligand (entries 3–4).

Table 4.8. *Cross-coupling of a less oxidized epoxide with a cyclic enol triflate.*

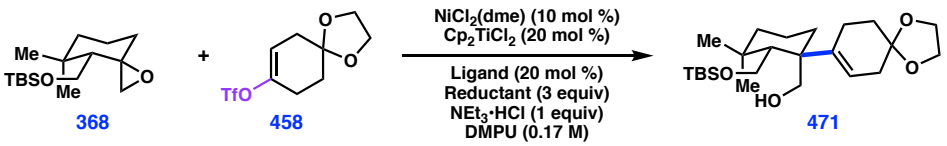

Entry	Ligand	Red.	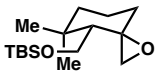 368	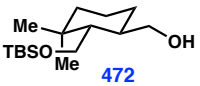 472	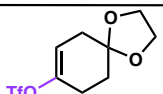 458	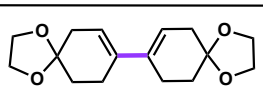 463
1	dtbpy	Mn	68 %	0 %	0 %	21 %
2	dtbpy	Zn	63 %	0 %	0 %	39 %
3	terpy	Mn	68 %	0 %	14 %	0 %
4	terpy	Zn	69 %	0 %	15 %	0 %
5	phen	Mn	83 %	0 %	0 %	36 %
6	phen	Zn	71 %	0 %	0 %	19 %

Disappointingly, we observed almost identical results with alkenyl iodide **460** in place of enol triflate **458** (Table **4.9**) with the less functionalized epoxide **368**. No conversion of the epoxide fragment to any other side product was detected under any of these conditions, and we observed analogous trends with regard to the C(sp^2) electrophile, with terpy delivering only recovered starting material (entries 3–4) and dtbpy and phen providing complete conversion to the divinyl side product (**463**) (entries 1–2, 5–6).

At this point, we wondered if we were using the wrong solvent for this reaction. While these reductive couplings with epoxide substrates have only been reported to react in DMPU, we decided to try additional solvents that had provided reactivity in the context of other reductive cross-couplings. We were particularly excited to try amide solvents, as we had had success using these solvents in the past and thought that these could potentially improve the desired reactivity.

We did not observe any notable reactivity with the epoxide substrate **368** in any of the solvents we tried (Table **4.10**). It seemed that as was the case in DMPU, the mass

balance with regard to the epoxide partner was just starting material. For the alkenyl cross-coupling partner, when we used MeCN or dioxane, we observed little to no conversion of the enol triflate electrophile (**458**) (entries 6 and 8). However, for each of the other solvents we explored, we saw complete conversion to the divinyl side product (**463**).

Table 4.9. *Cross-coupling of a less oxidized epoxide with a cyclic alkenyl iodide.*

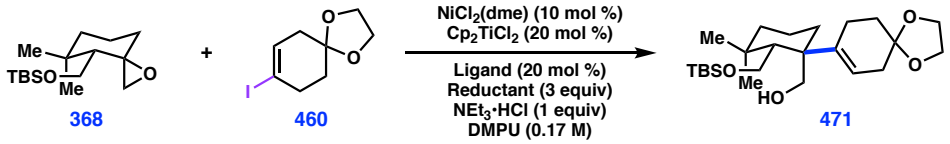

Entry	Ligand	Red.	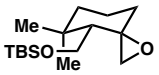 368	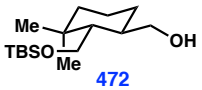 472	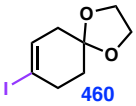 460	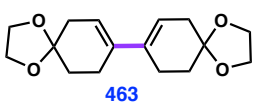 463
1	dtbpy	Mn	68 %	0 %	0 %	41 %
2	dtbpy	Zn	74 %	0 %	0 %	51 %
3	terpy	Mn	75 %	0 %	54 %	0 %
4	terpy	Zn	68 %	0 %	22 %	8 %
5	phen	Mn	64 %	0 %	0 %	38 %
6	phen	Zn	51 %	0 %	0 %	41 %

While there were certainly additional solvents we could explore in hopes of fine tuning the reduction potential of the titanocene we were using, we felt we had conducted an exhaustive exploration of the Weix conditions for the substrates we were interested in coupling, so we turned our attention toward cross-electrophile conditions that had been previously employed by Gong and coworkers to forge all-carbon quaternary centers. Unlike the Weix conditions, these reactions reported by Gong used a Ni(0) precatalyst, employed $MgCl_2$ as well as a pyridine base as additives, and instead used DMA as the solvent, rather than DMPU. We were particularly excited by their use of a nickel catalyst system to build sterically encumbered all-carbon quaternary centers, as we felt this was the most significant change between our system and the reported Weix system. We hoped that

by using a nickel catalyst that had been used to construct all-carbon quaternary centers in the reductive manifold, we could potentially forge the desired carbon-carbon bond using an epoxide as one of the electrophiles.

Table 4.10. *Solvent screen*

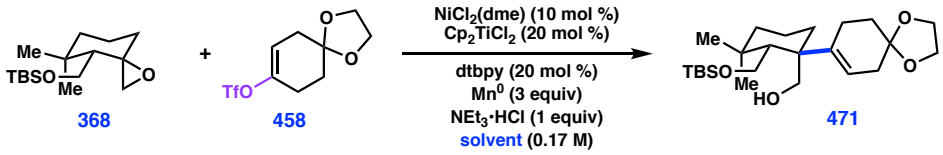

Entry	Solvent	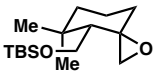 368	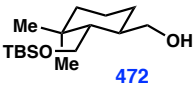 472	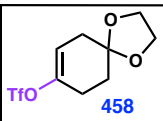 458	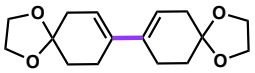 463
1	DMPU	70 %	0 %	0 %	38 %
2	DMF	67 %	0 %	0 %	29 %
3	DMA	66 %	0 %	0 %	33 %
4	MeOH	68 %	0 %	0 %	25 %
5	NMP	68 %	0 %	0 %	19 %
6	MeCN	74 %	0 %	46 %	0 %
7	THF	71 %	0 %	0 %	34 %
8	Dioxane	79 %	0 %	58 %	9 %

With this precedent in mind, we investigated the feasibility of this reaction using the Gong conditions. In conducting a broad survey of some of their most applicable conditions, we explored the reaction using $Ni(cod)_2$ and both the dtbpy and IPr ligands with different pyridine-based additives. Unfortunately, we observed disappointing results, again observing little to no reactivity of the epoxide substrate **368** (Table **4.11**). Use of the IPr ligands resulted in almost complete decomposition of **458** (entries 3–4). The combination of dtbpy as a ligand and DMAP as an additive provided significant quantities of the divinyl side product **463** (entry 1), while significant starting material was observed using dtbpy as the ligand with pyridine as an additive (entry 2).

Table 4.11. *Using the Gong conditions on our system*

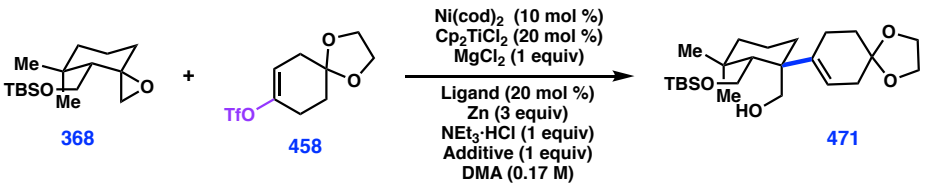

Entry	Ligand	Add.	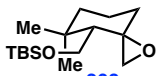 368	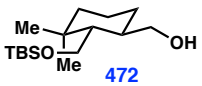 472	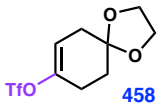 458	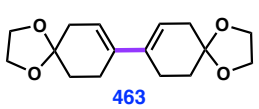 463
1	dtbpy	DMAP	85 %	0 %	0 %	34 %
2	dtbpy	Pyr	77 %	0 %	55 %	5 %
3	IPr	DMAP	85 %	0 %	0 %	1 %
4	IPr	Pyr	95 %	0 %	0 %	2 %

4.3 CONCLUDING REMARKS

After extensive exploration of both the intramolecular as well as the intermolecular cross-electrophile couplings of epoxide-containing substrates, we concluded that while simplifying and interesting, this strategy was not going to be viable in the context of the synthesis of the enmein-type *ent*-kauranoids. With this in mind, we turned our attention toward other approaches we could employ using some of the lessons we had learned throughout this investigation.

4.4 EXPERIMENTAL SECTION

4.4.1 Materials and Methods

General Procedures. Unless otherwise stated, reactions were performed in flame-dried glassware under a nitrogen atmosphere using freshly dried solvents. Methylene chloride (CH_2Cl_2), diethyl ether (Et_2O), tetrahydrofuran (THF), 1,4-dioxane, *tert*-butyl methyl ether (TBME), and toluene (PhMe) were dried by passing through activated alumina columns. Methanol (MeOH) was distilled over calcium hydride. Acetonitrile

(MeCN), *tert*-butanol (*t*-BuOH), anhydrous *N,N*-dimethylformamide (DMF), anhydrous *N,N*-dimethylacetamide (DMA), chloroform ($CHCl_3$), and absolute ethanol (EtOH) were used as received from Fisher Scientific. $NiBr_2$•dme and $Ni(cod)_2$ were purchased from Strem and stored in a N_2-filled glovebox. Zinc dust and Mangenese powder were purchased from Strem and stored in a dessicator. All other commercially obtained reagents were purchased from Sigma-Aldrich and used as received unless specifically indicated. All reactions were monitored by thin-layer chromatography using EMD/Merck silica gel 60 F254 pre-coated plates (0.25 mm). Silica gel and basic alumina column chromatography was performed as described by Still et al.[19] using silica gel (particle size 0.032–0.063) purchased from Silicycle and aluminum oxide (activated, basic, Brockmann I, 58 Å pore size, powder) purchased from Sigma-Aldrich. ^1H and ^{13}C NMR were recorded on a Varian Inova 600 (at 600 MHz), a Varian Inova 500 (at 500 MHz and 125 MHz respectively) or a Bruker Avance III HD with Prodigy cyroprobe (at 400 MHz and 101 MHz respectively). ^{19}F NMR spectra were recorded on a Varian Inova 400 (at 376 MHz). NMR data is reported relative to internal chloroform (^1H, $\delta = 7.26$, ^{13}C, $\delta = 77.2$) or to internal methanol (^1H, $\delta = 3.31$, ^{13}C, $\delta = 49.0$) and $PhCF_3$ (^{19}F, $\delta = -63.7$). Data for ^1H NMR spectra are reported as follows: chemical shift (δ ppm) (multiplicity, coupling constant (Hz), integration). Multiplicity and qualifier abbreviations are as follows: s = singlet, d = doublet, t = triplet, q = quartet, m = multiplet. IR spectra were recorded on a Perkin Elmer Paragon 1000 spectrometer and are reported in frequency of absorption (cm^{-1}). HRMS were acquired using either an Agilent 6200 Series TOF with an Agilent G1978A Multimode source in electrospray ionization (ESI), atmospheric pressure chemical ionization (APCI), or mixed

(MM) ionization mode. Specific optical rotations were recorded on a Jasco P-2000 polarimeter using a 100 mm cell.

4.4.2 Preparative Procedures and Spectroscopic Data

4.4.2.1 Substrate Synthesis

Preparation of epoxy alcohol **413**.

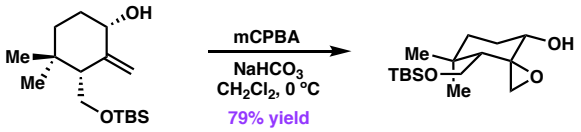

436 413

A 100 mL round bottom flask was charged with **436** (3.24 g, 11.4 mmol, 1 equiv). Then CH_2Cl_2 (57 mL, 0.2 M) was added, and the reaction mixture was cooled to 0 ºC. $NaHCO_3$ (4.783 g, 56.9 mmol, 5 equiv) was added in one portion followed by mCPBA (3.93 g, 17.1 mmol, 1.5 equiv, 75% mCPBA by weight). The reaction was allowed to stir for 2 minutes before it was quenched with saturated $Na_2S_2O_{3\,(aq)}$ (25 mL) followed by saturated $NaHCO_3$ (aq) (10 mL) and warmed to room temperature. The biphasic mixture was diluted with water (50 mL) and CH_2Cl_2 (50 mL). The aqueous phase was extracted with CH_2Cl_2 (3 x 50 mL). The combined organics were washed with saturated $Na_2S_2O_{3\,(aq)}$ (100 mL), saturated $NaHCO_3$ (aq) (3 x 100 mL), then brine (100 mL). The combined organics were dried over MgSO4, filtered, and concentrated *in vacuo*. The crude residue was purified by column chromatography using silica gel (10% EtOAc/hexanes → 15% EtOAc/hexanes) to give **413** (2.70 g, 79% yield) as an amorphous white solid.

$\mathbf{R}_f$ = 0.37 (silica gel, 20% EtOAc/Hex, CAM).

$[\alpha]_D^{23}$ = –17.5° (c = 0.65, $CHCl_3$).

^{1}H NMR (400 MHz, $CDCl_3$): δ 3.75 (dd, *J* = 10.5, 3.6 Hz, 1H), 3.63 (dd, *J* = 10.6, 4.1 Hz, 1H), 3.55 – 3.39 (m, 1H), 2.91 (d, *J* = 4.8 Hz, 1H), 2.69 (d, *J* = 4.8 Hz, 1H), 2.06 – 1.91 (m, 1H), 1.73 – 1.59 (m, 2H), 1.38 – 1.24 (m, 2H), 1.08 (s, 3H), 0.99 (s, 3H), 0.93 (s, 9H), 0.08 (d, *J* = 2.7 Hz, 6H).

^{13}C NMR (101 MHz, $CDCl_3$): δ 70.8, 61.0, 50.4, 48.7, 35.1, 29.9, 29.7, 28.4, 26.0, 26.0, 24.8, 18.2, -5.4, -5.6.

FTIR (NaCl, thin film, cm^{-1}): 3430, 2929, 2856, 1472, 1257, 1084, 837, 775.

HRMS (ESI-TOF, *m/z*): calc'd for $C_{16}H_{33}O_3Si$ $[M+H]^+$: 301.2193; found: 301.2196.

Preparation of β-ketoester **440**.

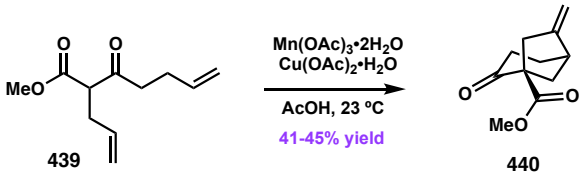

A flame-dried 250 mL round bottom flask was charged with freshly ground $Mn(OAc)_3•2H_2O$ (3 equiv, 12.3 g, 45.9 mmol) and $Cu(OAc)_2•H_2O$ (0.75 equiv, 2.29 g, 11.5 mmol). The flask was evacuated and back-filled with argon three times. The combined salts were suspended in degassed AcOH (75 mL, degassed by sparging with argon for 30 min). A separate flame-dried 50 mL pear-shaped flask was charged with **439** (3.00 g, 15.3 mmol, 1.0 equiv). This flask was evacuated and back-filled with argon three times, and then charged with degassed AcOH (12 mL, degassed by sparging with argon for 30 min). The solution of **439** was transferred to the 250 mL round bottom flask via cannula transfer

over the course of 20 minutes. The reaction mixture was allowed to stir for five hours, at which point the mixture was filtered over a pad of silica gel. The pad was washed with EtOAc (400 mL). The resulting blue solution was concentrated *in vacuo*, and then azeotroped with hexanes (3 x 100 mL) to remove some of the AcOH. The resulting blue solution was diluted with a 1:1 mixture of Et_2O/hexanes (300 mL), then washed with saturated NH_4Cl (aq) (150 mL). The organic layer was dried over $MgSO_4$, filtered, and concentrated *in vacuo*. The crude residue was purified by column chromatography using silica gel (5% EtOAc/hexanes → 10% EtOAc/hexanes, increasing by 1% EtOAc every 2 column volumes) to give **440** (1.18 g, 40% yield) as an amorphous pink solid with characterization data consistent with reports from Snider and coworkers.[14]

The enantiomers of **440** could be separated by chiral preparative HPLC. (IC, 20 x 250 mm, 200 μL injections, 10 mL/min, 20% IPA in hexanes, λ = 210 nm): t_R(–) = 23.72 min, t_R(+) = 26.16 min.

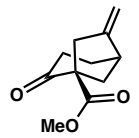

(–)-440, P1
t_R = 23.72 min
$[\alpha]_D^{23}$ = –173.0°
(c = 0.55, $CHCl_3$).

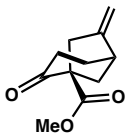

(+)-440, P2
t_R = 26.16 min
$[\alpha]_D^{23}$ = +219.5°
(c = 0.48, $CHCl_3$).

Preparation of acid **414**.

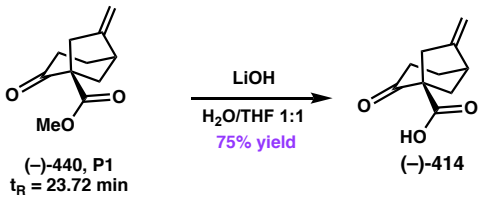

A 25 mL round bottom flask was charged with **440** (58.3 mg, 0.3 mmol, 1.0 equiv) and dissolved in THF (1 mL). The flask was submerged in an ice bath, and LiOH (22 mg, 0.9 mmol, 3.0 equiv) was added as a solution in water (1 mL). The reaction was stirred for 1.5 hours, at which point TLC indicated that no more starting material remained. The reaction was quenched with the addition of 5M HCl (600 μL). The mixture was diluted with water (3 mL) and then extracted with EtOAc (5 x 5 mL). The combined organics were dried over Na_2SO_4, filtered, and concentrated *in vacuo*. The crude residue was purified by column chromatography using silica gel (1% AcOH/1% MeOH/CH_2Cl_2 → 1% AcOH/2% MeOH/CH_2Cl_2) → 1% AcOH/3% MeOH/CH_2Cl_2 to give **414** (39.6 mg, 73% yield) as an amorphous colorless solid.

While we were able to use either (*S*) or (*R*) phenethylamine to perform a classical resolution to access each enantiomer of **414, this procedure was irreproducible. We elected to separate **440** by chiral preparative HPLC and hydrolyze each ester separately. Characterization data for each enantiomer of **414** is included below.

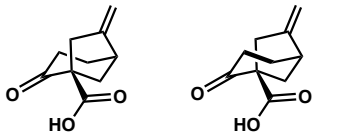

^{1}H NMR (400 MHz, $CDCl_3$): δ 10.64 (s, 1H), 5.09 (d, *J* = 2.2 Hz, 1H), 5.03 (s, 1H), 2.91 (dt, *J* = 18.0, 2.5 Hz, 2H), 2.71 (d, *J* = 17.7 Hz, 1H), 2.51 (ddd, *J* = 16.3, 11.5, 8.9 Hz, 1H), 2.40 (ddd, *J* = 16.3, 5.8, 2.1 Hz, 1H), 2.33 (ddd, *J* = 12.4, 5.1, 2.4 Hz, 1H), 2.03 (d, *J* = 12.2 Hz, 1H), 1.88 (ddd, *J* = 11.8, 6.1, 2.9 Hz, 2H).

^{13}C NMR (101 MHz, $CDCl_3$): δ 209.8, 176.2, 150.2, 108.1, 63.7, 41.7, 40.9, 39.6, 35.3, 33.4.

FTIR (NaCl, thin film, cm^{-1}): 2939, 1719, 1419, 1241, 1165, 1120, 1062, 899, 738.

HRMS (ESI-TOF, *m/z*): calc'd for $C_{10}H_{16}NO_3$ $[M+NH_4]^+$: 198.1125; found: 198.1120.

Synthesis of ester **443**.

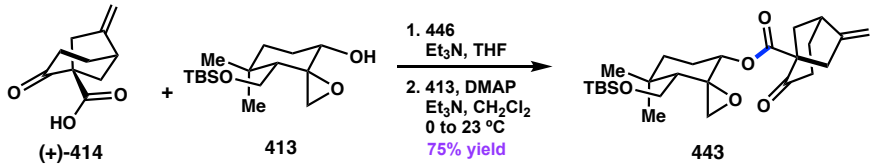

A 25 mL round bottom flask was charged with **(+)-414** (210 mg, 1.16 mmol, 1.0 equiv). The acid was azeotroped with PhMe (3 x 10 mL), then the flask was evacuated and back-filled with N_2 three times. The flask was then charged with THF (6 mL) and Et3N (244 μL, 1.75 mmol, 1.5 equiv). A solution of 2,4,6-trichlorobenzoyl chloride (**446**) (426 mg, 1.75 mmol, 1.5 equiv) was added as a solution in THF (3 mL) dropwise. After 3 hours, the reaction mixture was concentrated *in vacuo*, and the resulting residue was azeotroped

with PhMe (3 x 10 mL). The residue was then dried under high vacuum for five minutes, at which point **413** (350 mg, 1.16 mmol, 1 equiv) was added as a solution in benzene (3 mL), followed by DMAP (285 mg, 2.33 mmol, 2 equiv) as a solution in benzene (3 mL). The flask was then placed in a preheated oil bath and heated to 80 ºC. The mixture stirred for 1 hour, at which point the flask was removed from the oil bath and the reaction mixture allowed to cool to room temperature. The mixture quenched with the addition saturated $NaHCO_3$ (aq) (15 mL). The resulting mixture was diluted with water (15 mL) and EtOAc (15 mL). The aqueous layer was extracted with EtOAc (5 x 15 mL), and the combined organics were dried over Na_2SO_4, filtered, and concentrated *in vacuo*. The crude residue was purified by column chromatography using silica gel (5% EtOAc/hexanes → 6% EtOAc/hexanes) to give **443** (409 mg, 76% yield) as an amorphous, colorless solid.

R_f = 0.60 (silica gel, 20% EtOAc/Hex, p-anisaldehyde).

$[\alpha]_D^{23}$ = +51.5° (c = 0.27, $CHCl_3$).

^{1}H NMR (400 MHz, $CDCl_3$): δ 5.10 (d, *J* = 2.5 Hz, 1H), 5.03 (d, *J* = 2.1 Hz, 1H), 4.78 (dd, *J* = 7.6, 4.4 Hz, 1H), 3.75 – 3.58 (m, 2H), 3.00 – 2.87 (m, 1H), 2.86 – 2.66 (m, 4H), 2.50 (ddd, *J* = 16.0, 11.9, 8.7 Hz, 1H), 2.35 (dd, *J* = 16.0, 6.0 Hz, 1H), 2.25 (ddd, *J* = 12.4, 5.0, 2.7 Hz, 1H), 2.14 – 1.97 (m, 2H), 1.94 – 1.81 (m, 2H), 1.80 – 1.69 (m, 1H), 1.58 (d, *J* = 4.0 Hz, 1H), 1.10 (s, 3H), 0.99 (s, 3H), 0.86 (s, 9H), 0.02 (s, 3H), 0.02 (s, 3H).

^{13}C NMR (101 MHz, $CDCl_3$): δ 207.3, 170.3, 150.3, 108.2, 73.2, 64.5, 59.9, 58.1, 51.4, 49.3, 41.6, 40.3, 38.8, 35.3, 34.7, 33.5, 29.0, 26.4, 26.0, 25.4, 18.2, -5.3, -5.4.

FTIR (NaCl, thin film, cm^{-1}): 2955, 2858, 1743, 1715, 1472, 1291, 1258, 1156, 1061, 938, 838, 776.

HRMS (ESI-TOF, *m/z*): calc'd for $C_{26}H_{42}O_5Si$ $[M+H]^+$: 463.2874; found: 463.2868.

Synthesis of enol triflate **447**.

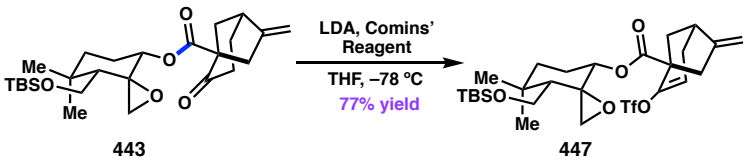

A 2-dram vial was charged with **443** (46.2 mg, 0.100 mmol, 1 equiv). The vial was evacuated and back-filled with nitrogen three times. The ester was dissolved in THF (500 µL) and cooled to –78 ºC. Then a solution of freshly prepared LDA (160 µL, 1.2 equiv, 0.75M) was added dropwise. The reaction was stirred at this temperature for 30 minutes, at which point Comins' reagent (45.2 mg, 0.115 mmol, 1.15 equiv) was added as a solid in one portion. After 4 hours, the reaction was warmed to room temperature and quenched by addition of water (2 mL). The mixture was diluted with saturated $NH_4Cl_{(aq)}$ (2 mL) and extracted with Et_2O (3 x 5 mL). The combined organics were washed with 3M NaOH (10 mL), pushed through a plug of Na_2SO_4, and then concentrated *in vacuo*. The crude residue was purified by column chromatography using silica gel (hexanes → 5% EtOAc/hexanes) to give **447** (45.6 mg, 77% yield) as an amorphous, colorless solid.

$\mathbf{R_f}$ = 0.63 (silica gel, 20% EtOAc/Hex, p-anisaldehyde).

$\mathbf{[\alpha]_D^{23}}$ = +10.2° (c = 2.3, $CHCl_3$).

^{1}H NMR (400 MHz, $CDCl_3$): δ 5.62 (dd, *J* = 4.8, 2.7 Hz, 1H), 5.12 – 4.96 (m, 2H), 4.79 (dd, *J* = 7.8, 4.4 Hz, 1H), 3.80 – 3.59 (m, 2H), 3.04 (dd, *J* = 16.4, 2.1 Hz, 1H), 2.95 (d, *J* = 4.5 Hz, 1H), 2.89 – 2.71 (m, 3H), 2.57 (ddd, *J* = 17.6, 4.3, 2.7 Hz, 1H), 2.23 – 2.10 (m, 3H), 2.11 – 1.95 (m, 1H), 1.85 – 1.67 (m, 1H), 1.54 (ddd, *J* = 13.8, 8.0, 4.1 Hz, 2H), 1.10 (s, 3H), 1.02 (s, 3H), 0.86 (s, 9H), 0.01 (s, 6H).

^{13}C NMR (101 MHz, $CDCl_3$): δ 169.5, 151.8, 149.5, 125.7, 118.0 ($J_{C–F}$ = 320 Hz) 115.9, 109.6, 73.9, 59.9, 58.1, 54.4, 51.4, 49.0, 43.6, 41.4, 39.3, 34.9, 34.7, 30.5, 29.8, 29.0, 26.2, 26.0, 18.2, -5.4, -5.5.

^{19}F NMR (282 MHz, $CDCl_3$): –73.6

FTIR (NaCl, thin film, cm^{-1}): 2929, 1743, 1420, 1292, 1236, 1213, 1164, 1143, 1079, 1046, 840, 775, 648

HRMS (ESI-TOF, *m/z*): calc'd for $C_{27}H_{45}F_3NO_7SSi$ $[M+NH_4]^+$: 612.2633; found: 612.2622.

Synthesis of epoxy ketone **465**.

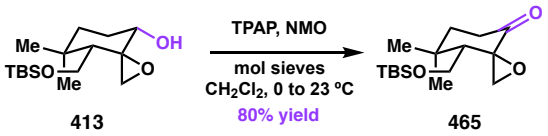

A 25 mL round bottom flask was charged with 4Å molecular sieves and flame-dried under vacuum for 3 minutes. The flask was allowed to cool under vacuum, and then back-filled with nitrogen at room temperature. Epoxy alcohol **413** (150 mg, 0.5 mmol, 1.0 equiv) was added, followed by NMO (88 mg, 0.75 mmol, 1.5 equiv). The solids were dissolved in CH_2Cl_2 (2.5 mL), and then the mixture was cooled to 0 ºC. TPAP (17.6 mg,

0.05 mmol, 0.10 equiv) was added in one portion. The reaction stirred at this temperature for one hour, at which point the flask was removed from the ice bath and allowed to stir at room temperature for 30 min. The mixture was pipetted directly onto an equilibrated silica gel column and purified directly via column chromatography (hexanes → 10% EtOAc/hexanes) to give **465** (119 mg, 80% yield) as a thick, colorless oil.

$\mathbf{R_f}$ = 0.53 (silica gel, 20% EtOAc/Hex, p-anisaldehyde).

^{1}H NMR (400 MHz, $CDCl_3$): δ 3.82 (dd, *J* = 10.6, 3.1 Hz, 1H), 3.70 (dd, *J* = 10.6, 3.7 Hz, 1H), 3.15 (d, *J* = 5.9 Hz, 1H), 2.86 (d, *J* = 5.9 Hz, 1H), 2.61 (ddd, *J* = 17.1, 8.6, 6.4 Hz, 1H), 2.48 (ddd, *J* = 17.1, 6.7, 6.2 Hz, 1H), 2.06 (ddd, *J* = 13.4, 8.6, 6.1 Hz, 1H), 1.68 (dtd, *J* = 13.3, 6.5, 1.2 Hz, 1H), 1.62 – 1.51 (m, 1H), 1.25 (s, 3H), 1.16 (s, 3H), 0.86 (s, 9H), 0.04 (s, 3H), 0.01 (s, 3H).

^{13}C NMR (101 MHz, $CDCl_3$): δ 206.1, 61.3, 60.2, 51.9, 50.6, 37.4, 37.3, 34.4, 28.9, 28.9, 26.2, 18.5, -5.4, -5.4.

4.4.2.2 Cross-Coupling Procedure

General Procedure for Cross-Couplings:

A 1-dram vial was charged with Et_3N•HCl, ligand, and reductant (if solid). The vial was then brought into a N_2-filled glovebox. Inside the box, the vial was charged with $TiCp_2Cl_2$ and then the nickel precatalyst. The vial was then charged with substrate(s) as a solution. The vials were sealed with a Teflon cap and brought out of the glovebox. The reactions were allowed to stir overnight at room temperature at 800 rpm. After 16 hours, the reactions were diluted with 20% EtOAc/Hexanes and pushed through a 6 cm plug of

SiO2 gel, eluting with 10 mL of 20% EtOAc/Hexanes. The solvent was removed *in vacuo*, and 1,2,4,5-tetrachloro-3-nitrobenzene was added. The yields of each product were determined by ^{1}H-NMR spectroscopy.

4.5 NOTES AND REFERENCES

(1) Cha, J. Y.; Yeoman, J. T. S.; Reisman, S. E. *J. Am. Chem. Soc.* **2011**, *133*, 14964.
(2) Yeoman, J. T. S.; Mak, V. W.; Reisman, S. E. *J. Am. Chem. Soc.* **2013**, *135*, 11764.
(3) Yeoman, J. T. S.; Cha, J. Y.; Mak, V. W.; Reisman, S. E. *Tetrahedron* **2014**, *70*, 4070.
(4) Cherney, A. H.; Kadunce, N. T.; Reisman, S. E. *J. Am. Chem. Soc.* **2013**, *135*, 7442.
(5) Cherney, A. H.; Reisman, S. E. *J. Am. Chem. Soc.* **2014**, *136*, 14365.
(6) Kadunce, N. T.; Reisman, S. E. *J. Am. Chem. Soc.* **2015**, *137*, 10480.
(7) Poremba, K. E.; Kadunce, N. T.; Suzuki, N.; Cherney, A. H.; Reisman, S. E. *J. Am. Chem. Soc.* **2017**, *139*, 5684.
(8) Suzuki, N.; Hofstra, J. L.; Poremba, K. E.; Reisman, S. E. *Org. Lett.* **2017**, *19*, 2150.
(9) Hofstra, J. L.; Cherney, A. H.; Ordner, C. M.; Reisman, S. E. *J. Am. Chem. Soc.* **2018**, *140*, 139.
(10) Zhao, Y.; Weix, D. J. *J. Am. Chem. Soc.* **2014**, *136*, 48.
(11) Zhao, Y.; Weix, D. J. *J. Am. Chem. Soc.* **2015**, *137*, 3237.
(12) Wang, X.; Wang, S.; Xue, W.; Gong, H. *J. Am. Chem. Soc.* **2015**, *137*, 11562.
(13) Uroos, M.; Hayes, C. J. *Org. Lett.* **2010**, *12*, 5294.
(14) Dombroski, M. A.; Kates, S. A.; Snider, B. B. *J. Am. Chem. Soc.* **1990**, *112*, 2759.
(15) Inanaga, J.; Hirata, K.; Saeki, H.; Katsuki, T.; Yamaguchi, M. *Bull. Chem. Soc. Jpn.* **1979**, *52*, 1989.
(16) Shiina, I.; Kubota, M.; Ibuka, R. *Tetrahedron Lett.* **2002**, *43*, 7535.
(17) At the time, we were unaware of the absolute configuration of **414** we were obtaining through the chiral resolution. Unfortunately, we later discovered that these experiments were carried out using the incorrect diastereomer shown.
(18) Overman, L. E.; Tanis, P. S. *J. Org. Chem.* **2010**, *75*, 455.
(19) Still, W. C.; Kahn, M.; Mitra, A. *J. Org. Chem.* **1978**, *43*, 2923.